

INVESTIGATION INTO CRACKING OF A WELD REPAIRED TURBINE CASING

by
G. Das,
N. K. Mukhopadhyay,
S. Ghosh Chowdhury &
D. K. Bhattacharya

Material Characterization Division,
National Metallurgical Laboratory,
Jamshedpur 831007, India

Presented at the Silver Jubilee Seminar '98 of the IIW, Calcutta Branch on 17-18 April '98. Theme : Welding – Its productivity, Quality Control & Value Engineering.

ABSTRACT

The present study was aimed at analysing the failure of a weld repaired turbine casing after 30 years of total service including 5 years after weld repair. The casing was weld repaired by a high alloyed weld metal (24Cr-32Ni-4Mn-Fe). The base metal consisting of ferrite-pearlite microstructure did not show any appreciable degradation during service. δ ferrite was observed at the interface of weldment and HAZ as predicted by the Schaeffler diagram. The δ -ferrite phase appeared to transform to alloy carbides and σ -phase during high temperature service.

The difference between thermal expansion coefficients of ferritic and austenitic stainless steel led to the generation of stress in addition to the usual thermal stress. The resultant stress was estimated to be near to the yield stress indicating that the weld zone experienced a typical condition of low cycle fatigue. The presence of striations on the fracture surface confirmed thermal fatigue as the failure mode. Crack growth took place along the grain boundaries

embrittled by σ -phase and led to failure. The correct choice of the filler metal should have been a high Ni-base alloy having similar coefficient of thermal expansion as the ferritic steel base metal.

INTRODUCTION

Casing is one of the major components of a turbine system [1]. High pressure steam from boiler is fed into the casings through nozzles to rotate the turbine discs. The casing withstands the steam pressure as well as maintains support and alignment of the internal components. It is normally a massive cast structure with a large wall thickness. Increased efficiency requires higher steam pressures and temperatures; thus, requiring casing materials with improved thermal fatigue resistance as well as greater toughness and high yield strength. In general, the class of materials more extensively used for casing are Cr-Mo steels i.e. low alloy ferritic steels. The strength of these steels at elevated temperature is derived from the effect of solid solution and alloy carbide precipitation [2].

High pressure turbine casings are prone to two types of damages : distortions and cracking. Casing distortion can cause damage by allowing contact between stationary and rotating parts. Distortion is caused due to thermal gradient and rapid start-stop cycles. Secondly, high thermally stressed zones are critical for crack initiation. Cracking of the casing leads to steam leakage and in extreme situation to bursting. Cracking can be caused by three reasons : thermal fatigue (65%), brittle fracture (30%) and creep (5%) [3]. Most electrical supply systems operate on a load following mode and thus, are dependent on daily and seasonal variation in load. This leads to transient thermal gradients during load cycle. Repeated cyclic stresses aided by creep damage at high temperature lead to the formation of cracks. These cracks are normally transgranular in nature; degradation of material toughness due to long term service exposure results in rapid crack growth and catastrophic brittle failure can then take place. Therefore, it is necessary to remove the cracks by grinding at the early

stages and local repairs be carried out by welding [4-7].

In the present case, the cracking in a repair welding zone in a turbine casing of 60 MW thermal power plant has been investigated. The turbine assembly had two zones : (a) High pressure (HP) zone and low pressure (LP) zone. After 25 years of service, a crack was detected on the lower casing of HP zone near the steam inlet. This crack was repaired by welding. After 5 years of service since the repair, a crack was again detected on the weld zone. The thickness of the casing made up of a Cr-Mo steel was of the order of 0.50 m. The size of the crack was 0.10 m in radial direction and 0.30 m in axial direction. A schematic diagram showing the crack morphology is shown in Fig. 1. Actual photograph showing the crack in the turbine casing is not shown on ac-

count of a confidentiality agreement with the power plant authority. In the present paper, the causes of cracking of the weld zone have been analyzed. The present condition of the base metal has also been evaluated to assess whether the turbine can be employed again after repairing the new crack.

For the purpose of analysis, a piece (0.06 m x 0.02 m) was trepanned from the cracked region.

EXPERIMENTAL PROCEDURE

The composition of the base metal and weld metal were determined by standard spectrometric analysis. Metallography was carried out as per standard practice. The microstructure was analyzed by scanning electron microscope (SEM) equipped with energy dispersive X-ray analysis (EDX) facility. Special etching method was employed to detect the

presence of δ -ferrite in the weld zone. It was done by chemical etching with boiling Murakami's reagent for 5 minutes. The composition of the reagent is 10 gm $K_3Fe(CN)_6$, 10 gm KOH and 100 ml distilled water. To reveal σ -phase, electrochemical etching was carried out with a solution of 40 gm NaOH and 100 ml distilled water. A constant voltage source was used with platinum foil as cathode. Voltage was 3V and the time of etching was 35 sec.

Fractography was carried out by SEM to understand the mode of fracture. Hardness testing was performed in a Vickers scale in order to estimate the yield stress and tensile stress of the base and weld metal using standard formulae of conversion.

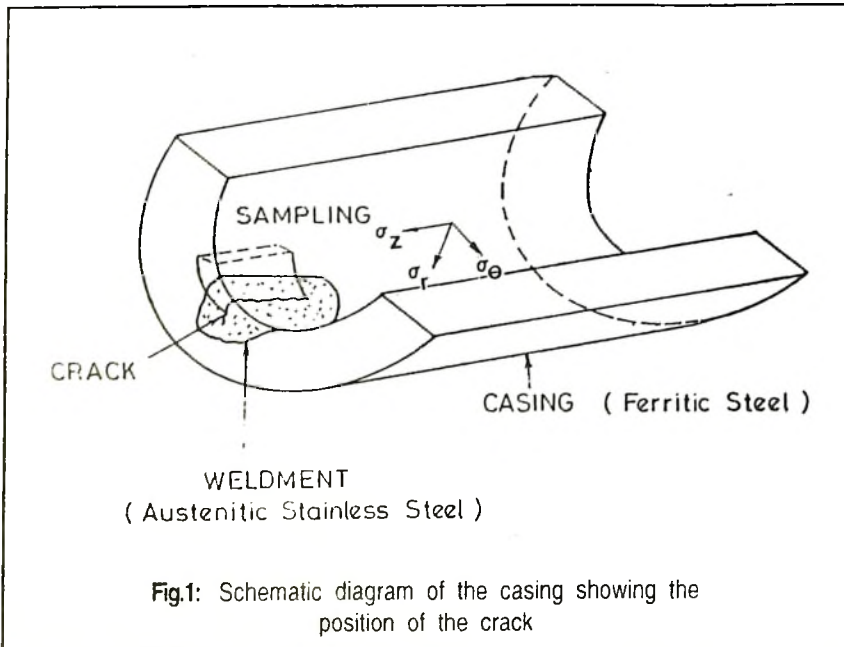
RESULTS

Visual Examination

Fig. 2 shows the photomicrograph of the piece cut from the fractured zone of the casing. Three zones were identified in the figure namely, weldmetal, Haz, and the base metal. A hole can be observed on the weld region. Cracks were found to have emanated from that hole.

Chemical Analysis

The casing material was found to be 1 Cr-0.5 Mo type with 0.18% carbon. The weld metal was found to be : 0.18%C, 0.32%Si, 4%Mn, 24%Cr, 32%Ni, 2%Mo, ~ 1%Nb and balance Fe. This corresponds to an austenitic alloy equivalent to modified 800H[8].



Microstructure

Microstructure of the base metal shows ferrite-pearlite structure (Fig. 3) which is expected from this grade of steel under a normalised condition [9]. Pearlite colonies started to break up, but the process of disintegration was yet to be complete fully. Fine particles of carbides were also seen within the ferrite grains. Some elongated carbides were observed at the grain boundary. By EDX, it was found that cementite in the pearlite colony is enriched with other alloying elements i.e. Mn, Cr, Mo. The carbides within the grain could not be analyzed by SEM because of their small size. However, as per literature, those fine precipitates should be complex alloy carbides [9].

Microstructure of weld metal showed cellular morphology (Fig.4). Microcracks were found to have nucleated from the hole. Cracks were also observed along the austenite grain boundaries. The cracks were mostly intergranular in nature (Fig. 5). EDX analysis showed the presence of Cr rich phase along the grain boundary. Nb was also found in this region. It is known that Si and Nb in addition to the impurity elements, S, P segregate at the dendrite interfaces during solidification causing cracking [10]. δ -ferrite was not observed in the weldment; except near the weld/base metal boundary on the weld metal side at the austenite grain boundaries (Fig. 6). σ -Phase was also observed at

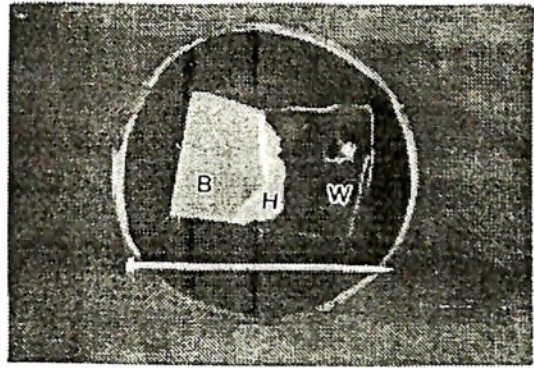


Fig.2: Macrostructure showing the various zones of the sample across the weldment (W:Weld Zone; H:HAZ; B:Base Metal)

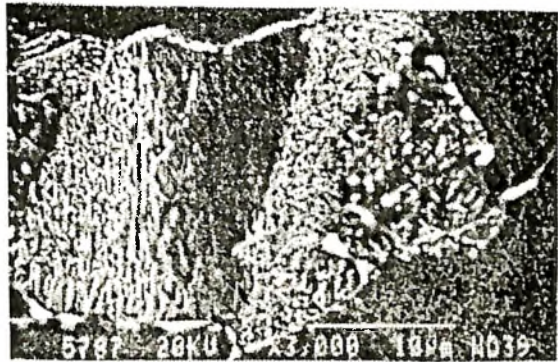


Fig.3: Microstructure of the base metal

the grain boundary in the weldment very near to HAZ (Fig. 7). HAZ also showed the presence of σ -phase at the ferrite grain boundary (Fig. 8).

Fractography

SEM investigation of the fractured surface showed that the cracks had originated within the weld zone. The voids and cavities observed in the

weld zone appeared to be the sites of crack origin. These voids and cavities might have been generated during the welding operation due to improper welding procedure. Diffuse striations were observed in the fracture surface (Fig. 9). These diffuse striations can be attributed to be a signature of thermal fatigue.

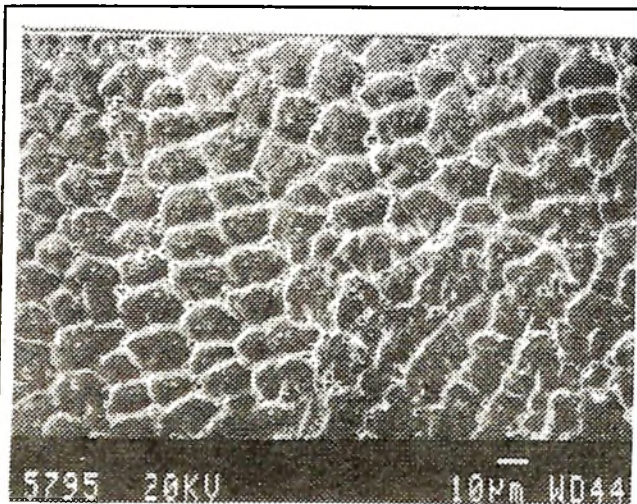


Fig.4: Cellular microstructure of the weld metal

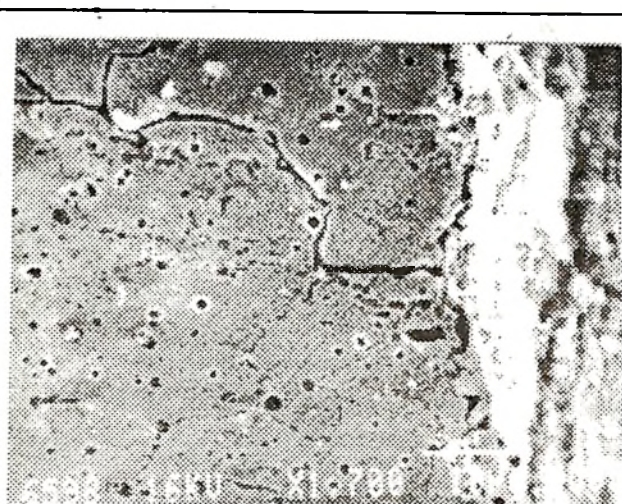


Fig.5: Intergranular crack propagating from a hole present in the weldment

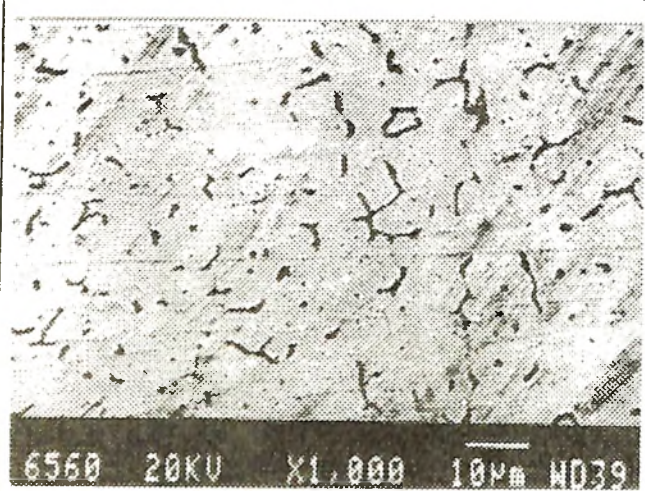


Fig.6: Presence of δ -ferrite within the weld very near to weld/HAZ interface

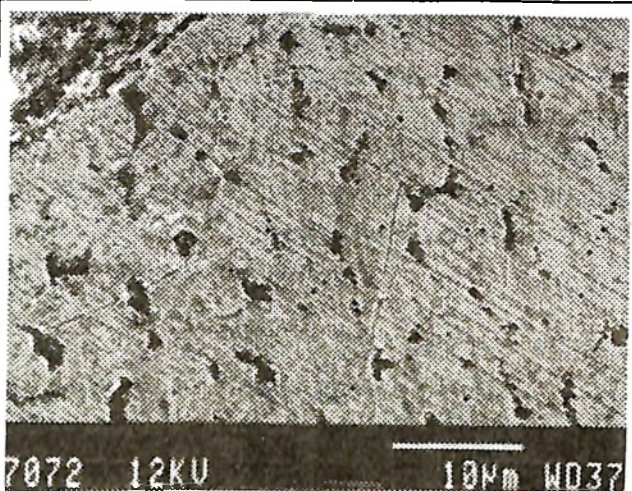


Fig.7: Presence of σ -phase at the austenite grain boundary in the weld.

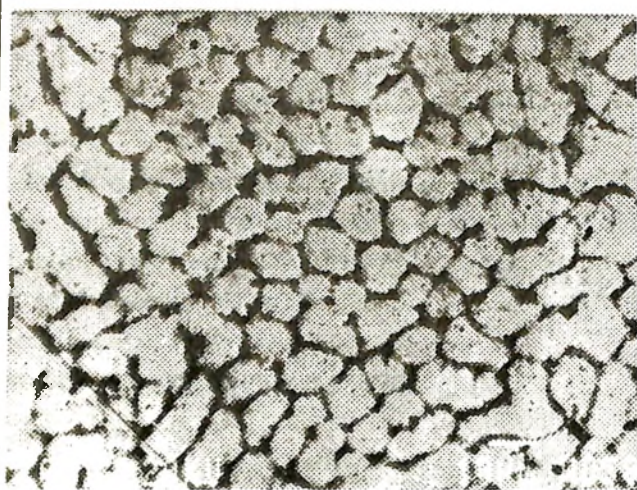


Fig.8: Presence of σ -phase at the ferrite grain boundary in HAZ



Fig.9: Diffuse striations observed at the fracture surface

Hardness

Hardness measurements (VHN-20kg) were carried out on the base metal as well as on the weldment. The values in the base metal was found to be 190-200 which is expected from this steel of the microstructure described earlier. Hardness values obtained at the weldment showed large scatter (300-400 VPN).

The tensile stress in MPa was estimated from hardness data by the following relationship [11] : $\delta_{TS}(\text{MPa}) \approx 3.2 \times \text{Hv}$. The values were 624 MPa for base metal and 960 MPa for weld metal.

DISCUSSION

It is necessary to understand the following points in order to analyze the failure in the repaired weld joint :

- a) Is the base metal in good metallurgical condition
- b) Was the choice of the austenitic alloy as the repair weld filler metal proper
- c) If the choice of the filler metal was not correct, what could have been a better choice

For a repair weld, the first condition to satisfy is that the filler metal must show a good weldability. The second requirement is that the ductility of the weld metal and the HAZ should be equal if not better than the base metal.

The material for welding was austenitic. For a high temperature service,

the characteristics of the filler metals and base metal should ideally be matched as closely as possible. Thus, 1.25Cr - 0.5Mo filler metal can be used for welding 0.5Cr - 0.5Mo, 1Cr - 0.5Mo and 1.25Cr - 0.5Mo steels [12]. However, after welding, the components should be annealed to relieve residual stress since such steels undergo martensitic/bainitic transformation during welding, if preheating is not carried out. The tendency for martensite formation is reduced to a considerable extent and even eliminated when austenitic steel is used as filler metal.

For a large component like casing, preheating and postweld heating are difficult. To avoid such heat treatment of thicker section, austenitic stainless steel of AISI 309 or 310 are often employed for minor repair welding of Cr-Mo steels [12]. Stainless steel weld metal has higher as-welded ductility than Cr-Mo steel. For these reasons, the majority of welding stresses are relieved through yielding during the welding operations. It also resists decarburization and thermal shock. As austenitic steels are richer in alloying elements, the weld metal near the fusion line gets diluted and the HAZ gets enriched in alloying elements. The dilution effect is important since the microstructure in steel or metallic alloy is a function of the chemical composition and the heating/cooling rates. This, in a way, can reduce the susceptibility for martensite formation.

Another reason for the use of austenitic steel is the susceptibility of ferritic steels to type IV cracking i.e. cracking during post-weld heat treatment [13]. This cracking occurs at the edges of HAZ material adjacent to unaffected base metal. Improved heat treatments have been found to eliminate the propensity for type IV cracking. However, it requires furnace facilities capable of implementing the stress-relief treatment of the entire component. Otherwise, the only alternative is to incorporate a 10 to 20% safety margin of stress into the design.

The above points of discussion suggest that repair welding of low alloy ferritic steel by austenitic filler metal is easier at inaccessible regions of service induced cracks by avoiding the preheating and the post weld heat treatments. However, it has been found that this austenitic filler metal is not satisfactory if the welded joint is subjected to cyclic temperature service or a service temperature where either C-migration or σ -phase formation can take place [12]. In the present case, chemical analysis of the base metal and the weldment have shown that the amount of carbon is same in both the cases (0.18%). Hence, the possibility of C-migration can be ruled out. Therefore, the role of σ -phase was very important.

Condition of the Base Metal

In the case of the ferrite-pearlite microstructure the cementite platelets

break up and gradually spheroidise at high temperature. Partitioning of alloying elements like Cr, Mo also takes place between the matrix and the carbides. There have been several investigations to understand the nature of microstructural changes and consequent degradation. In terms of the morphology and size of carbides that we have observed, the microstructure in the base metal matches with the Grade "C" of the table by Toft & Marsden [15]. This is as follows : "Intermediate stage of spheroidization; distinct signs of carbide spheroidization in the pearlite areas although lamellar nature is still evident. Increased carbide precipitation within the ferrite grains as well as along the grain boundaries". Grade 'C' lies intermediate between grade 'A' and 'F'. This indicates that the base metal still retains a microstructure that should not lead to failure. The question then is - why the base metal developed a crack in the first place when the repair was carried out earlier. A possibility is that a defect was present from the manufacturing stage that had initiated the crack.

Condition of the Weld metal

From the chemical analysis, the weld metal was found to be closer to modified 800H [8]. This alloy contains Nb which helps to have an increase in corrosion resistance and retain high strength at moderately high temperature. Also, the presence of Nb increases the resistance to sensitization during welding or

service exposure at high temperatures [16, 17]. The alloy has similar thermal conductivity in comparison to austenitic steels; but the thermal expansion coefficient is intermediate between the austenitic stainless steels and the ferritic steels [18].

It has long been recognised that austenitic stainless steels are subject to cracking in either the weld metal or the heat affected zone (HAZ) or in both [19]. The type and origin of cracking has been associated with the low liquation temperature of various microstructural constituents [20]. The problem is also known to be severe in thick sections because of greater constraint [21]. Recently, liquation cracking in the HAZ of AISI 347 was found to be associated with eutectics of Nb

rich phases at grain boundaries or interfaces [22].

To assess the worth of alloy 800H as a filler metal, Schaeffler diagram (Fig. 14) can be made use of. The chromium and nickel equivalents in the X and Y axis in the diagram are calculated as follows :

$$Cr_{eq} = \%Cr + \%Mo + 1.5 (\%Si) + 0.5(\%Nb) \text{ and}$$

$$Ni_{eq} = \%Ni + 30(\%C) + 0.5(\%Mn)$$

On this basis, the low alloy ferritic steel in the present case corresponds to the point 'P' ($Cr_{eq} = 1.55$, $Ni_{eq} = 5.9$) and that of the weld metal corresponds to point 'Q' ($Cr_{eq} = 27.23$ and $Ni_{eq} = 39.4$) in the diagram (Fig. 10). Since point 'P' lies in the martensite region and point 'Q' lies in the fully austenite region, there is a

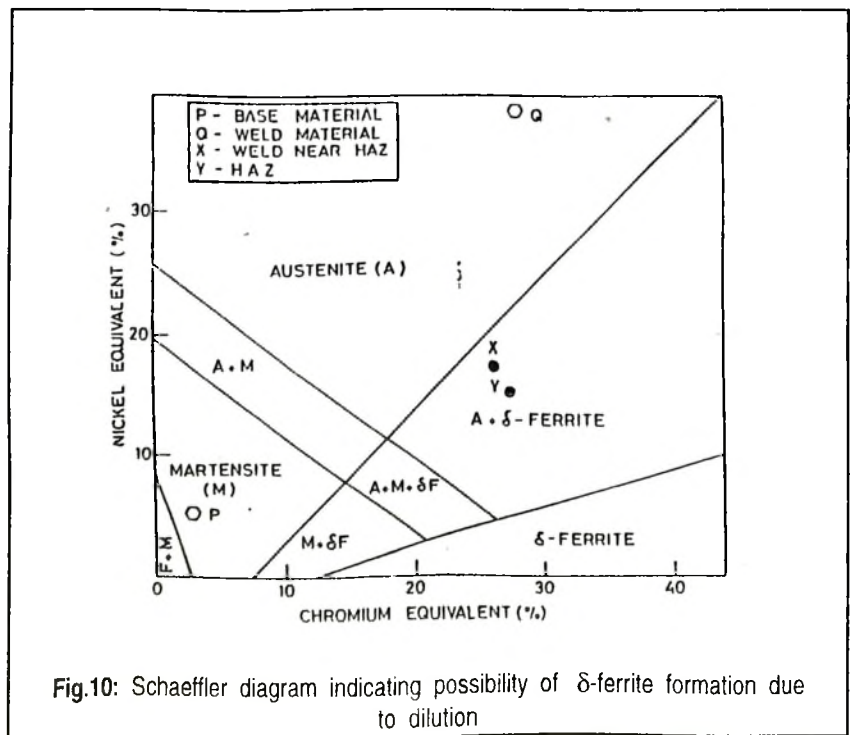


Fig.10: Schaeffler diagram indicating possibility of δ -ferrite formation due to dilution

possibility of a large amount of dilution by the base metal when it melts during the weld metal deposition. It has been estimated from the diagram that in order to have a microstructure which would have martensite phase other than austenite, a dilution of the order of 65% is needed. For fully martensite, a dilution of 77% is required. Practically, the amount of dilution mentioned above is impossible to achieve. But to have δ -ferrite as a secondary phase, the required dilution would be much less and achievable.

Fully austenitic steel is liable to hot cracking which occurs during weld metal solidification. This cracking takes place due to segregation of impurity elements such as S, P and other elements lead to low melting point phases. It is well known that the δ -ferrite in the HAZ or weld in austenitic steels benefits resistance to hot cracking. Certain amount of δ -ferrite (5-8vol%) will scavenge the impurities and take care of certain amount of thermal strain [23]. While the primary reason for hot cracking is segregation of deleterious elements at the grain boundaries, an important contributing factor is the high coefficient of thermal expansion due to which a large amount of strain accumulates during solidification of the weld metal. Schaeffler diagram is a good pointer to indicate the solidification mode of stainless steels.

The cracks that have been observed in the weld metal in the present case

could be due to one or more of the following reasons : (i) hot cracking as explained above, (ii) due to transformation of δ -ferrite to σ -phase; the δ -ferrite could be formed during welding, and (iii) due to thermal fatigue damage. Hot cracking as mentioned earlier is due to the presence of impurities at the grain boundaries; however, such elements were not detected. Hence, the presence of hot cracking by impurity can be ruled out. However, the second possibility i.e. transformation of δ -ferrite cannot be ruled out. According to Schaeffler diagram, the weld metal is in the fully austenitic region. Also, by using boiling Murakami's reagent as an etchant, no δ -ferrite was observed in the weldment. However, δ -ferrite was observed near the HAZ (within the weldment) as well as within the HAZ. The volume fraction of δ -ferrite was more in the HAZ. The formation of this phase can be explained if the effect of dilution can be taken into account. Migration of Cr is prominent among the other species because of its size factor. Cr having the smallest atomic diameter can diffuse easily compared to Ni and Mo. On the basis of EDX analysis the weld metal near HAZ had $Cr_{eq} > 25$ and $Ni_{eq} < 20$. Similar analysis shows that HAZ had $Cr_{eq} > 30$ and $Ni_{eq} < 15$. The above two cases are marked as X and Y, respectively in the Schaeffler diagram (Fig. 14). As Cr_{eq} increases and Ni_{eq} decreases, the propensity of δ -ferrite formation increases.

EDX analysis at the austenite grain boundaries showed considerable amount of second phases which are enriched with Nb. Nb being more reactive compared to Cr, forms more stable carbides or carbonitrides. Constitutional liquation of these compounds occur in Nb bearing austenitic alloys to form a low melting point eutectic with austenite [22]. It has been observed metallographically by Messler and Li [24] that a eutectic of austenite and Nb rich phase was present at the final stages of solidification of the liquated grain boundaries in an austenitic steel. They also showed similar behaviour of significant Nb enrichment at the grain boundary compared to the matrix. It was reported that a high C+N content relative to Nb content increased the liquation temperature of grain boundary eutectic, reducing cracking susceptibility. However, in the present case, Nb content is quite high and that lowered the liquation temperature and increased the cracking susceptibility, probably by forming Fe₂Nb.

After high temperature exposure the δ -ferrite converts to σ -phase and alloy carbides by two step eutectoid reactions [25]. The first step leads to the formation of austenite and a Cr-rich carbide (M₂₃C₆) by a lamellar eutectoid reaction. σ -phase forms as a result of a second eutectoid reaction. Once the σ -phase forms, the microcracks formed due to thermal stress will propagate fast with the aid

of σ -phase embrittlement. Even voids can generate near the grain boundary carbides as well as around the σ -phase. In the following discussion, the intensity of thermal fatigue to initiate cracks within the weldment will be analyzed.

Origin of Stress

Two types of stresses are mainly found in the casing e.g. thermal stress due to temperature cycling and mechanical stress due to the steam pressure. In the following sections, the following stress components are considered: σ_θ the circumferential stress, σ_z the longitudinal stress, and σ_r the radial stress (Fig. 1).

Considering the solution of thermal stress in a hollow cylinder with inner and outer radius, a , and b , respectively, the stress components are as follows [26].

$$\sigma_z = \frac{\alpha E}{1-\nu} \left(\frac{2}{b^2 - a^2} \int_a^b T r dr - T \right) \quad (1)$$

α is the coefficient of thermal expansion, ν is the poisson's ratio, E is the Young's modulus, r is the point from the centre where the stress is to be calculated and T is the temperature. Considering steady temperature distribution and T_a , T_b as the inner and outer surface temperatures, the distribution of temperature as a function of r from the centre can be expressed as :

$$T = T_b + \Delta T \frac{\log \frac{b}{r}}{\log \frac{b}{a}} \quad (2)$$

Here, ΔT is equal to $(T_a - T_b)$. Putting the above expression in stress equations, the relations at any distance (r) from the centre of the cylinder can be expressed as :

$$\sigma_\theta = \frac{\alpha_F \cdot E \cdot \Delta T}{2(1-\nu) \cdot \log \left(\frac{b}{a} \right)} \left[1 - \log \frac{b}{a} - \frac{a^2}{b^2 - a^2} \left(1 + \frac{b^2}{r^2} \right) \log \frac{b}{a} \right] \quad (3)$$

$$\sigma_z = \frac{\alpha_F \cdot E \cdot \Delta T}{2(1-\nu) \cdot \log \left(\frac{b}{a} \right)} \left[1 - 2 \log \frac{b}{r} - \frac{2a^2}{b^2 - a^2} \log \frac{b}{a} \right] \quad (4)$$

$$\sigma_r = \frac{\alpha_F \cdot E \cdot \Delta T}{2(1-\nu) \cdot \log \left(\frac{b}{a} \right)} \left[- \log \frac{b}{r} - \frac{a^2}{b^2 - a^2} \left(1 + \frac{b^2}{r^2} \right) \log \frac{b}{a} \right] \quad (5)$$

where α_F is the thermal expansion coefficient for the ferritic steel.

It can be seen from the above equations that if ΔT is positive (which is the case during heating), the radial stress, σ_r is compressive at all points and becomes zero at the inner as well as outer surfaces. The stress components of σ_θ and σ_z have their maximum compressive values at the inner surface ($r = a$) and maximum tensile values at the outer surface ($r = b$). The values of those stresses at the two surfaces are equal in magnitude. Now it is of interest to evaluate those stresses at $r = a$ where the stress components are reduced to

$$(\sigma_\theta)_{r=a} = (\sigma_z)_{r=a} = \frac{\alpha E \Delta T}{2(1-\nu) \cdot \log \left(\frac{b}{a} \right)} \left[1 - \frac{2b^2}{b^2 - a^2} \log \frac{b}{a} \right] \quad (6)$$

The casing is about 50 cm thick. Inside wall temperature which is in contact with the steam is around 400°C whereas outer is at around 200°C. Taking $\alpha_F = 12 \times 10.6/^\circ\text{C}$; $E = 160 \text{ GPa}$, $\Delta T = 200^\circ\text{C}$ (This value has been estimated from the theoretical considerations of temperature of steam, thermal conductivity and heat flux), $\nu = 0.3$, $a = 0.70 \text{ m}$ and $b = 1.20 \text{ m}$, the values of σ_θ and σ_z are found to be 343 MPa.

Austenitic weldmetal has high thermal expansion coefficient (α_A) of $18 \times 10^{-6}/^\circ\text{C}$ around 500°C compared to the ferritic steel ($\alpha_F = 12 \times 10^{-6}/^\circ\text{C}$) [18]. Therefore, the effect due to this thermal mismatch must be considered for evaluating the stresses. It is possible to approximate the thermal stress that might be generated at the inner surfaces due to this mismatch. The value of E for both the filler material as well as the base material have been considered to be equal. Comparing the thickness of the cylinder with respect to the depth of the weld zone, the above stress equations can be modified as

$$\sigma_\theta = \sigma_z = \frac{M}{Z} = \frac{(\alpha_A - \alpha_F) \cdot \Delta T \cdot E}{2(1 - \nu)} \quad (7)$$

The stress values are evaluated to be of 136 MPa. Hence, the total stresses arising out of thermal stress are in the order of 480 MPa.

The stresses generated due to steam pressure ($-6 - 8$ MPa) during heating cycle can be neglected in comparison with the stress values of thermal origin. Now applying Tresca's criterion, with the above stress condition at the inner surface, where σ_θ and $\sigma_z = -480$ MPa and $\sigma_r = 0$, the equivalent stress is found to be of 480 MPa which is nearer to the yield stress of the material. It should be noted that similar magnitude of stress will develop during heating and cooling cycle leading to a situation of low cycle fatigue. The defects present in the weld will act

as stress raiser and eventually crack will be initiated in the weldment by thermal fatigue (low cycle fatigue) mechanism. It is highly probable that after a few cycles crack will be initiated under the above stress condition and will propagate fast if weak paths are available in the microstructure. In the present case, a weak path was present in the form of σ phase at the grain boundaries.

CONCLUSIONS

The weld repaired zone in a ferritic steel turbine casing developed crack again due to a wrong choice of the filler metal for the repair. The base metal consisting of ferrite-pearlite microstructure did not show any appreciable amount of spheroidization. However, the weldment was found to be degraded. Dilution of alloying elements took place and δ ferrite was observed at the interface of weldment and HAZ in line with the prediction by Schaeffler diagram. These δ -ferrites appeared to transform to alloy carbides and σ phase during high temperature service exposure. The difference between thermal expansion coefficients of ferritic and austenitic stainless steel led to the generation of stress in addition to the thermal stress. The resultant stress (480 MPa) was found nearer to the yield stress which indicates that the weld zone experienced a situation of low cycle fatigue. Holes and cavities which had been present in the weld appeared to be responsible for initiating the cracks. The presence of striations

on the fracture surface confirmed thermal fatigue as the failure mode. Cracks after the initiation from the defects, grew faster along the austenite grain boundary embrittled by σ phase and led to failure of the component.

The correct choice of the filler metal should have been a high Ni-base alloy having similar coefficient of thermal expansion as the ferritic steel base metal.

ACKNOWLEDGEMENT

Authors wish to acknowledge Mr. Swapan K. Das, Dr. G. Sridhar, Dr. S. Tarafdar, Dr. N. Parida and Mr. Rajeev Kumar for stimulating discussions and assistance in carrying out various experiments. Authors are thankful to Mr. D. Sanyal and Mrs. S. Mukhopadhyay for useful discussions on thermal stress-analysis. Authors are grateful to Prof. P. Ramachandra Rao, Director, National Metallurgical Laboratory, Jamshedpur for his kind permission to publish this paper.

REFERENCES

1. Modern Power Station practice, "British Electricity International", Pergamon Press, Third edition (1992).
2. R. G. Baker and J. Nutting, JISI, July, 257 (1959).
3. R. Viswanathan, Damage mechanisms and Life Assessment of High Temperature Components, ASM International, Metals Park, Ohio, 308 (1989).
4. S. J. Brett. Materials Development in Turbo-Machinery Designs, The In-

- stitute of Metals, London, 166 (1989).
5. Y. Sugita, T. Sugiura, T. Fujiwara and K. Tomoda, First Intl. Conf. on Microstructure and Mechanical Properties of Aging Materials, TMS, 91 (1993).
 6. D. Yosh and A. Caploon, Welding J., 71(2), 29 (1992).
 7. T. J. David, in Thermal Stress and Thermal Fatigue, ed. D.J. Litter, Butterworths, London 185 (1969).
 8. R. Viswanathan, Damage Mechanisms and Life Assessment of High Temperature Components, ASM International, Metals Park, Ohio, 410, cf 32 (1989).
 9. J. Orr, F.R. Beckett and G.D. Fawkes, Ferritic Steel for fast reactor steam generators, BNES, London, 91 (1975).
 10. V. Shankar, T.P.S. Gill, S.L. Mannan and P. Rodriguez, Internal report IGC-119, Indira Gandhi Centre for Atomic Research (1991).
 11. D.R.H. Jones, Engineering Materials 3, Pergamon Press, London, 358 (1993).
 12. Welding Handbook, ed. W.H. Keans, vol. 4, 53 (1984).
 13. R.T. Townsend, Advances in Materials Technology for Fossil Fuel Power Plants, eds. R. Viswanathan and R.I. Jaffee, ASM, Metals Park, Ohio, 11 (1987).
 14. R. Viswanathan, ASTM J. Test Eval., 3, 93 (1975).
 15. L.H. Toft and R.R. Marsden, Cong, Structural processes in creep, JISI/ JIM, London (1963).
 16. R.J. Christoffel, Weld J., 39(7), 315 (1960).
 17. E. Folkward, Welding metallurgy of stainless steel, Boston, MA, Springer-Verlag, 209 (1987).
 18. V.K. Sikka, Status and Development and Commercialization of Modified 9Cr-1Mo Steel, Internal Report, Oak Ridge National Laboratories, May 24 (1979).
 19. ASM Handbook, ASM Metals Park, Ohio, 6, 500, 686 (1993).
 20. T.M. Cullen and J.W. Freeman, Trans ASME, J. Engg. Power, 85, 151 (1963).
 21. R.D. Thomas, Jr, Weld J., 63 (12), 24, 355 (1963).
 22. R.W. Messler, Jr and L.Li, Science and Tech. Welding and Joining, 2 (2), 43, cf 23 (1997).
 23. W.L. Fleischmann, Weld J., 33 (9), 459 (1954).
 24. R.W. Messler, Jr and L.Li Science and Tech. Welding and Joining, 2 (2) 43 (1997).
 25. C.C. Tseng, S.W. Thompson, G. Krauss, Y. Shen and M.C. Mataya, Metall. Trans., 25A, 1147 (1994).
 26. S.P. Timoshenko and J.N. Goodier, Theory of Elasticity, McGraw Hill, London, 448 (1970).



*With Best Compliments from :
The official Printer of
The Indian Institute of Welding*

BUSINESS CLUB

HOUSE OF REPROGRAPHICS

**7A, Bentinck Street, 1st Floor,
Calcutta 700 001
Phone : 248 7640
Fax : 91 33 2481623**

*With Best Compliments from :
The official Courier of
The Indian Institute of Welding*



Bom-Ind Courier

DOMESTIC & INTERNATIONAL

6/1, Burtolla Street, 2nd Floor, Calcutta - 700 007 Tel : 232 4132